

Neurofibromatosis-1 regulates neuroglial progenitor proliferation and glial differentiation in a brain region-specific manner

Da Yong Lee, Tu-Hsueh Yeh, Ryan J. Emnett, Crystal R. White, and David H. Gutmann

Supplemental Material

Table S1

“Table S1”, List of antibodies used for immunocytochemistry (ICC) and immunohistochemistry (IHC)

Table S2

“Table S2”, List of antibodies used for Western blotting

Table S3

“Table S3”, List of primers used for real-time quantitative RT-PCR

Supplemental materials and methods

Supplemental reference

Figure S1, related to Figure 1

Figure S2, related to Figure 1

Figure S3, related to Figure 2

Figure S4, related to Figure 2

Figure S5, related to Figure 3

Figure S6, related to Figures 5, 6 and 7

Table S1. Antibodies used for immunocytochemistry (ICC) and immunohistochemistry (IHC) (Ms[§]: mouse antibody; Rb*: rabbit antibody)

Antibody	Antigen retrieval	Source	Dilution
BLBP (ICC, IHC), Rb*	citrate buffer (pH=6.0)	Chemicon, Temecula CA	1:1000
APC (CC1) (IHC), Ms [§]	citrate buffer (pH=6.0)	Calbiochem, San Diego CA	1:50
Clusterin(IHC), Rb	citrate buffer (pH=6.0)	Santa Cruz, Santa Cruz CA	1:100
Cre (IHC), Ms	citrate buffer (pH=6.0)	Novagen, Madison WI	1:10000
GFAP (ICC), Rb	none	Sigma, St Louis MO	1:500
GFAP (IHC), Rat	1 mM EDTA (pH=8.0)	Zymed, San Francisco CA	1:200
GFP (IHC), Rb	citrate buffer (pH=6.0)	Abcam, Cambridge MA	1:2500
Nestin (ICC), Ms	none	Calbiochem	1:100
NeuN (IHC), Ms	citrate buffer (pH=6.0)	Chemicon	1:250
NG2 (IHC), Rb	1 mM EDTA	Chemicon	1:100
O4 (ICC), Ms (IgM)	none	Chemicon	1:1000
Olig2 (ICC, IHC), Rb	citrate buffer (pH=6.0)	Charles D. Stiles (Dana Farber)	1:10000
PDGFR- α (IHC), Rat	citrate buffer (pH=6.0)	BD Pharmingen, Franklin Lakes NJ	1:100
Tuj-1 (ICC), Ms	none	Covance, Berkeley CA	1:1000
WT-1 (IHC), Rb	citrate buffer (pH=6.0)	Abcam	1:100

Table S2. Antibodies used for Western blotting (Ms[§]: mouse antibody; Rb*: rabbit antibody)

Antibody	Host	Source	Dilution
4EBP1	Rb*	Cell Signaling , Denver MA	1:1000
Akt	Rb	Cell Signaling	1:1000
Cre	Ms [§]	Covance	1:10000
FoxO1	Rb	Cell Signaling	1:1000
GSK3- β	Rb	Cell Signaling	1:1000
H-Ras	Rb	Santa Cruz	1:200
K-Ras	Rb	Santa Cruz	1:200
MAPK	Rb	Cell Signaling	1:1000
Neurofibromin	Rb	Santa Cruz	1:250
N-Ras	Ms	Santa Cruz	1:200
p120-GAP	Ms	BD Transduction Laboratory	1:2000
p27	Rb	Cell Signaling	1:1000
p68	Rb	Jason D. Weber (Washington University School of Medicine)	1:10000
phospho-4EBP1	Rb	Cell Signaling	1:1000
phospho-Akt	Rb	Cell Signaling	1:1000
phospho-FoxO1	Rb	Cell Signaling	1:1000
phospho-GSK-3 β	Rb	Cell Signaling	1:1000
phospho-MAPK	Rb	Cell Signaling	1:1000
phospho-p27 (Ser10)	Rb	Zymed	1:200
phospho-p27 (T198)	Rb	Abcam	1:1000
phospho-PDK1	Rb	Cell Signaling	1:1000
phospho-PKC α	Rb	Cell Signaling	1:1000
phospho-S6	Rb	Cell Signaling	1:1000
phospho-S6 Kinase	Rb	Cell Signaling	1:1000
phospho-STAT3	Rb	Cell Signaling	1:1000
PKC α	Rb	Cell Signaling	1:1000
PTEN	Rb	Cell Signaling	1:1000
Raptor	Rb	Bethyl Laboratories, Montgomery TX	1:1000
Rictor	Rb	Bethyl Laboratories	1:1000
S6	Rb	Cell Signaling	1:1000

S6 Kinase	Rb	Cell Signaling	1:1000
STAT3	Rb	Cell Signaling	1:1000
pan Ras	Ms	Upstate Biotech, Billerica MA	1:10000
α -tubulin	Ms	Sigma	1:10000

Table S3. Primers used for real-time quantitative RT-PCR

Gene	Accession #	Forward primer	Reverse primer
<i>Ppp2r2b</i>	NM_028392	5'- ATGGAATGGGTCAGACAGCG-3'	5'- GGCCTCAAGGGTCACATCAC-3'
<i>Prkce</i>	NM_011104	5'- CACCAGCACGGAGTGATCTACA-3'	5'- CCTTGCACATCCCAAAGTCAG-3'
<i>Prkcq</i>	NM_008859	5'- ATGCATGTGGCATGAACGTC-3'	5'- ATCATCGCTAGTGCTTCAGCC-3'
<i>Rasa2</i>	NM_177644	5'- ACAGGAAAAGCGGATCGTGT-3'	5'- ATTGCGGACCTGCATGCT-3'
<i>Rasgrp1</i>	NM_011246	5'- ATCTTTTGATGCGGATGGAAA-3'	5'- TAGCAGCTCGGCTGAGGAG-3'
<i>Tenc1</i>	NM_153533	5'- GGCTGATGAGCGGTTTCCT-3'	5'- AGAGGGATCATTCCGTGGG-3'
<i>Actb</i>	NM_007393	5'-ACTATTGGCAACGAGCGGTT-3'	5'-ATGCCACAGGATTCCATACCC-3'

Supplemental Experimental Procedures

Sectioning of neurospheres for immunocytochemistry. Neurospheres were fixed in 4% paraformaldehyde for 30 min followed by washing twice in PBS. Neurospheres were cryoprotected with 30% w/v sucrose solution for 3-4 hr (von Holst et al., 2006). Fixed neurospheres were embedded in freezing medium and sectioned at 16 μ m.

Multi-lineage differentiation assay. Neurospheres were trypsinized and plated onto 24 well plates coated with poly-D-lysine (50 μ g/ml) and fibronectin (10 μ g/ml) with NSC medium without growth factors. After 6 days, the cells were fixed with 4% paraformaldehyde. For optic nerve (ON) neurospheres, single neurospheres were plated onto poly-D-lysine- and fibronectin-coated plates without trypsinization.

Ras activity assay. The levels of GTP-bound active Ras were measured by Raf1-RBD affinity chromatography using the Ras activity assay kit (Upstate Biotechnology, Lake Placid, NY) according to the manufacturer's instructions. Briefly, 150 μ g of protein was incubated with agarose beads conjugated with Raf1-RBD for 50 min at 4°C. Raf1-RBD bound Ras isoforms were detected by Western blotting using anti-K-, H- and N-Ras isoform-specific antibodies.

Measurement of NSC self-renewal and proliferation. At least 10 neurospheres from each genotype were trypsinized and plated into individual wells of ultra-low binding 24 well plates with complete NSC medium containing EGF and FGF. After 12-14 days, NSC self-renewal was assessed by counting the number of resulting secondary neurospheres. Supplements were added every 3 days. To measure NSC proliferation over several passages, 5000 cells from each genotype beginning at passage 3 were plated into individual wells. Resulting neurospheres were trypsinized and cell number was counted at day 6. This procedure was repeated for a total of three passages.

Real-time quantitative reverse transcription-PCR (qRT-PCR). Real-time qRT-PCR was performed as previously described (Yeh et al., 2009) using the primers listed in **Table S3**. β -actin was used as an internal control. For each gene, the $\Delta\Delta CT$ values were calculated for each gene from at least three independently-generated PN1 NSC cultures.

Supplemental Reference

von Holst A, Sirko S, Faissner A. 2006. The unique 473HD-Chondroitinsulfate epitope is expressed by radial glia and involved in neural precursor cell proliferation. *J Neurosci* **26**: 4082-4094.

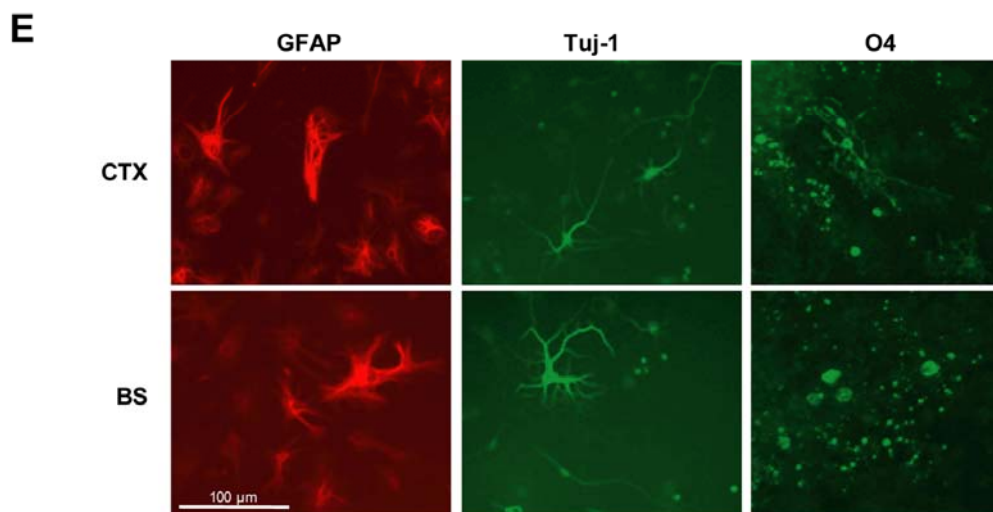
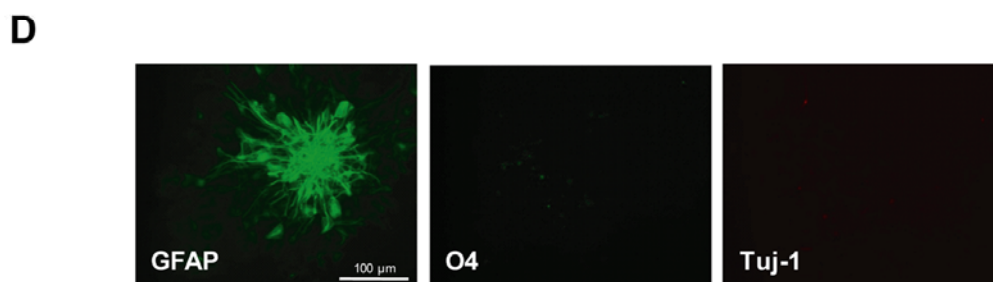
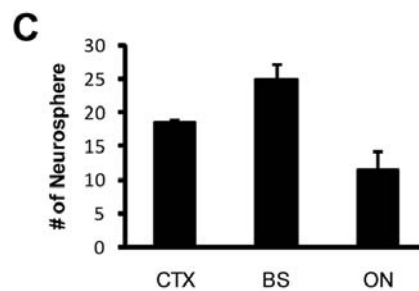
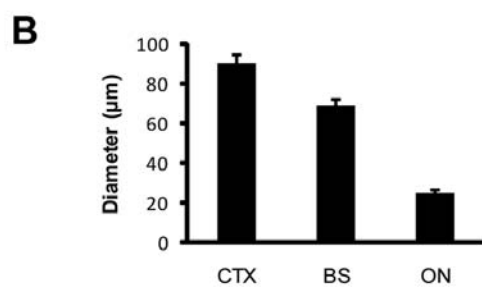
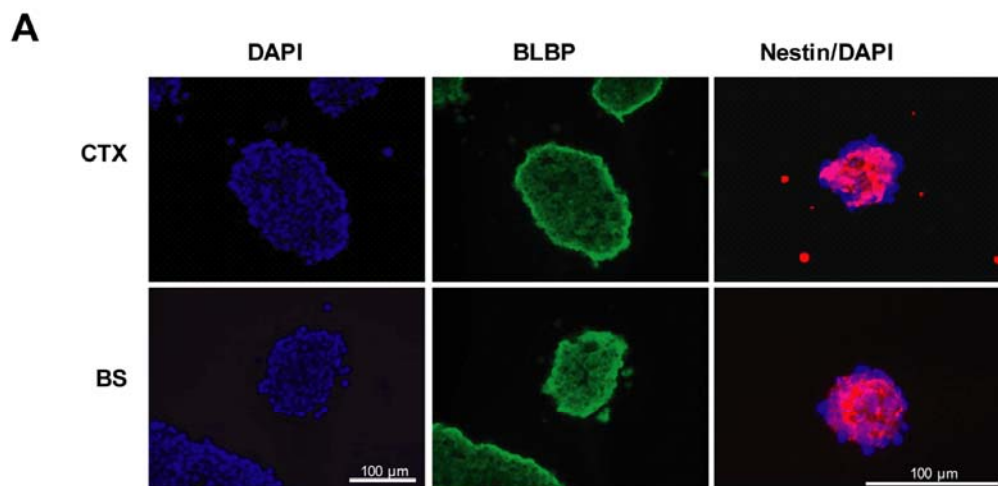


Fig. S1. Characterization of NSC cultures from different brain regions. (A) Neurospheres generated from the CTX or BS of PN1 mice were positive for BLBP and nestin expression. Cells were counterstained with DAPI. Quantification of the size (B) and the number (C) of secondary neurospheres generated from single neurospheres from the neocortex (CTX), brainstem (BS) and optic nerve (ON) shows that NSCs from different brain regions exhibit different levels of self-renewal and proliferation. (D) Multi-lineage differentiation of ON neurospheres revealed that most of the cells differentiated into GFAP+ astrocytes, but not Tuj-1+ neurons or O4+ oligodendrocytes. (E) Multi-lineage differentiation of PN1 NSCs from the CTX and BS is shown. Immunocytochemistry with Tuj-1 (neuron), GFAP (astrocyte) and O4 (oligodendrocyte) antibodies shows that PN1 NSCs from both the CTX and BS can differentiate into these three different types of brain cells. Scale bar: 100 μ m.

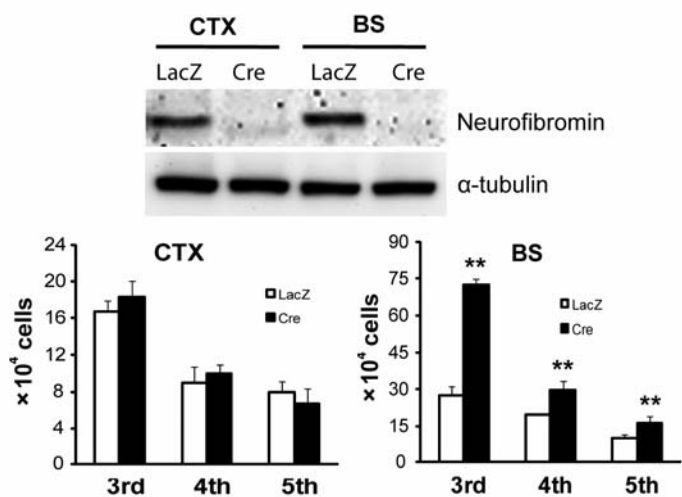
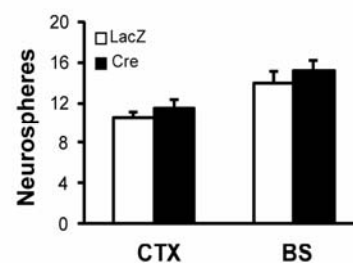
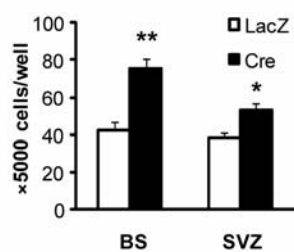
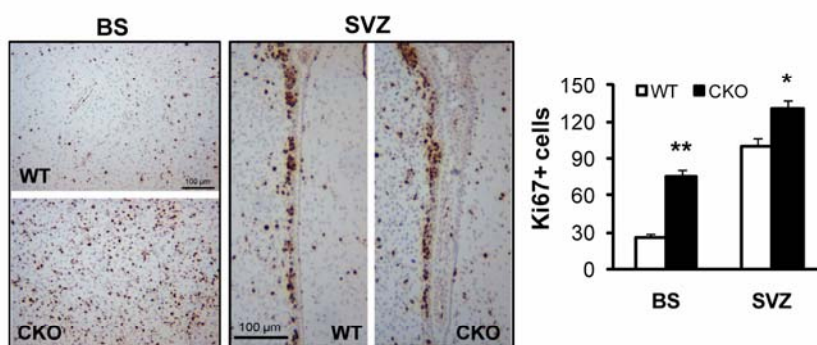
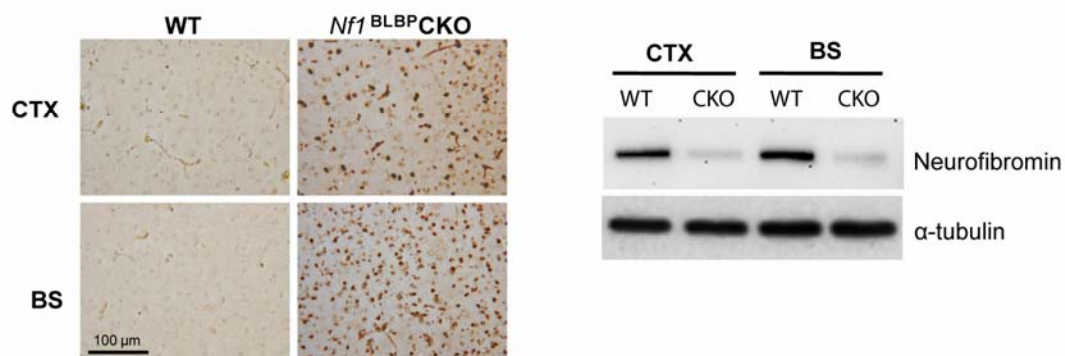
A**B****C****D****E**

Fig. S2. Increased proliferation in BS NSCs was observed following *Nf1* gene inactivation.

(A) Direct cell counting over several passages shows increased proliferation of NSCs only from the BS, but not the CTX, following *Nf1* inactivation. *Nf1* gene inactivation was confirmed by Western blotting (top). (B) No change in self-renewal was observed in *Nf1*^{-/-} NSCs compared to WT NSCs. (C) Direct cell counting revealed a 1.4-fold increase in PN1 SVZ NSC proliferation relative to WT NSCs. (D) The number of Ki67⁺ cells in the SVZ of PN8 *Nf1*^{BLBP}CKO mice was increased by 1.3-fold compared to WT control littermates. (E) Loss of neurofibromin following Cre expression was confirmed by Cre immunohistochemistry using an anti-Cre antibody (left) and neurofibromin western blotting (right) in both the CTX and the BS of PN18 *Nf1*^{BLBP}CKO mice. Scale bar: 100 μ m. Values represent mean \pm SEM. * $p < 0.05$, ** $p < 0.01$.

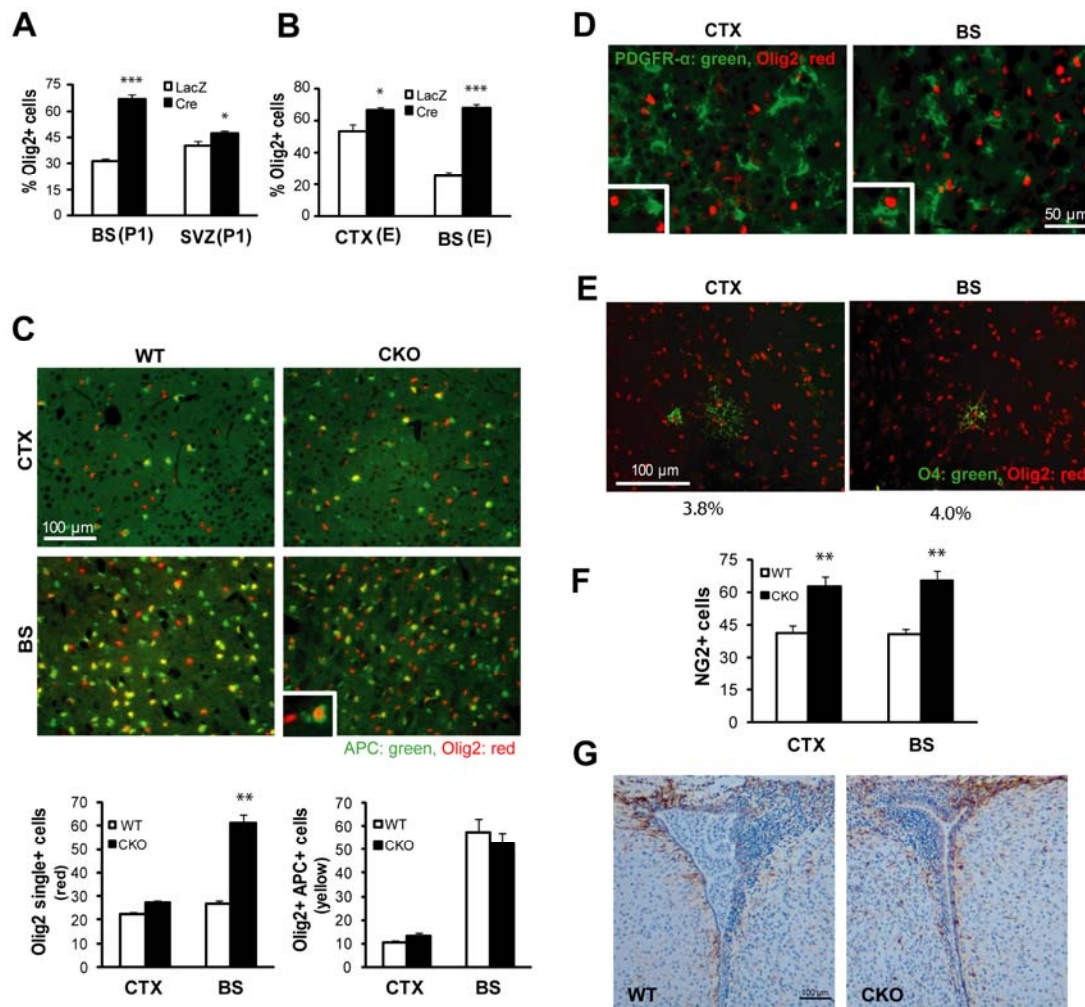


Fig. S3. Olig2+ cells are increased in the brainstem following *Nf1* loss. (A) The number of Olig2+ cells was increased by 2.2-fold in PN1 BS NSCs following *Nf1* inactivation compared to 1.4-fold in PN1 SVZ NSCs. (B) The number of Olig2+ cells was increased by 2.7-fold in embryonic (E16) BS NSCs following *Nf1* inactivation compared to 1.3-fold in E16 CTX NSCs. (C) Double immunofluorescence immunocytochemistry for APC (CC1) and Olig2 shows that while the number of Olig2+ (red) cells was increased following *Nf1* inactivation in the BS, there was no change in the number of APC/Olig2 double positive (yellow) cells. (D) The majority of the Olig2+ cells in the CTX and BS of PN8 *Nf1*^{BLBP}CKO mice were not positive for PDGFR-α. (E) Fewer than 5% of the Olig2+ cells were O4+ following *in vitro* differentiation of *Nf1*-deficient CTX (3.8%) and BS (4.0%) NSCs. (F) The number of NG2+ cells was increased in both CTX (1.5-fold) and BS (1.6-fold) of *Nf1*^{BLBP}CKO mice compared to WT controls. (G) No change in the number of GFAP+ cells was observed in the SVZ of *Nf1*^{BLBP}CKO mice compared to WT controls. Scale bar: (C, E, G), 100 μm; (D), 50 μm. Values represent mean ± SEM. *p<0.05, **p<0.01, ***p<0.0001.

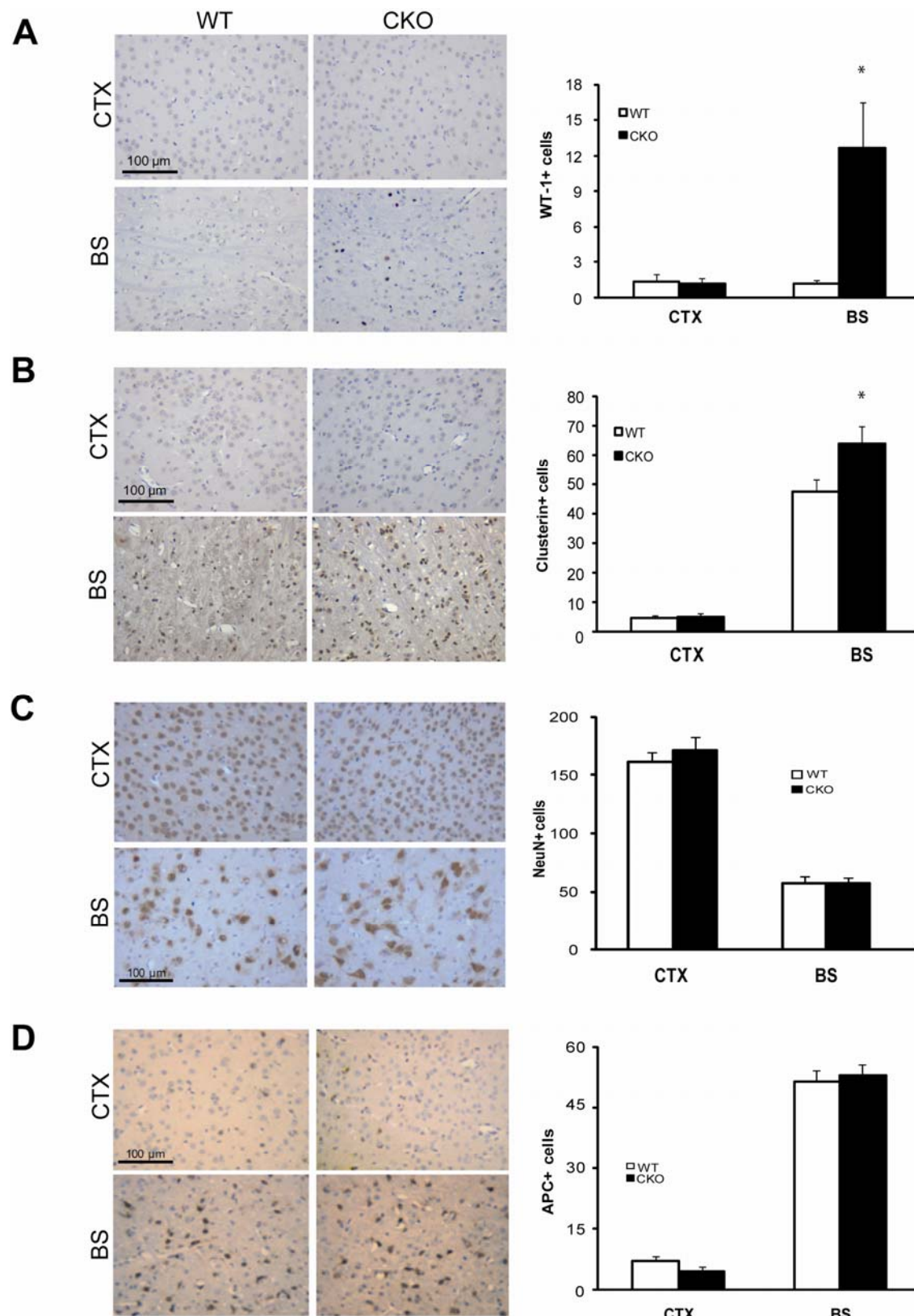


Fig. S4. *Nf1* loss affects only astroglial lineage differentiation *in vivo*. The number of WT-1- (A) and clusterin- (B) positive astrocytes was increased in the BS of PN18 *Nf1*^{BLBP}CKO mice compared to wild-type (WT) controls. No changes in astrocyte cell numbers (WT-1+ or clusterin+ cells) were observed in the CTX following *Nf1* inactivation. (C) NeuN immunohistochemistry demonstrates that *Nf1* loss does not change the number of NeuN+ neurons in the PN18 *Nf1*^{BLBP}CKO mouse brain. (D) There was also no difference in the number of APC+ oligodendrocytes between PN18 WT and *Nf1*^{BLBP}CKO brains. Scale bar: 100 μ m. Values represent mean \pm SEM. *p<0.05.

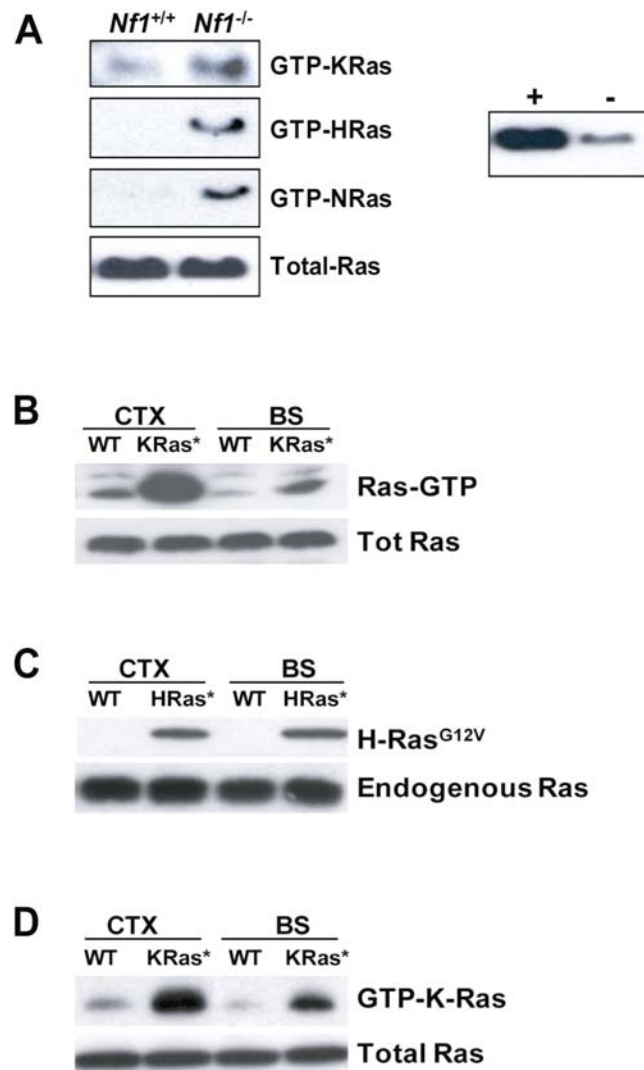


Fig. S5. Ras transgene expression and activation. (A) *Nf1*^{-/-} embryonic (E11.5) NSCs exhibit increased levels of GTP-bound (activated) K-Ras, H-Ras, and N-Ras relative to WT NSC cultures. For positive (+) and negative (-) controls, cell lysates were incubated with 100 μ M GTPyS and 1 mM GDP, respectively. (B) GTP-bound activated Ras was increased in BLBP-Cre; LSL-K-Ras^{G12D} (KRas^{*}) mouse brain tissues relative to WT brains. (C) Expression of constitutively-active H-Ras was confirmed by Western blotting in MSCV-H-Ras^{G12V}-GFP (HRas^{*})-infected NSC cultures. (D) Expression of constitutively-active K-Ras was detected using a Ras activity assay followed by Western blotting with anti-K-Ras antibody in K-Ras^{G12D} (KRas^{*})-expressing NSCs.

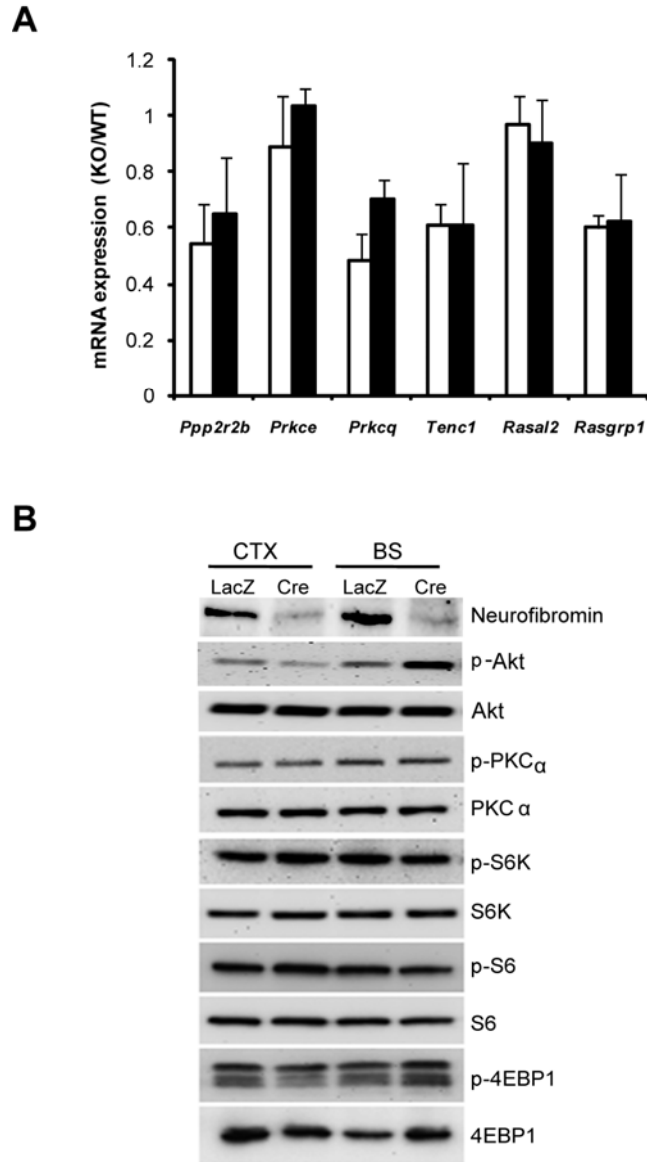


Fig. S6. Neurofibromin loss in BS and CTX NSCs has no effect on the expression of upstream Ras and Akt regulators or mTOR downstream effectors. (A) mRNA expression levels of *Ppp2r2b* (protein phosphatase 2), *Prkce* (PKC ϵ), *Prkcq* (PKC θ), *Tenc1* (C1-TEN), *Rasal2* (Ras protein activator like 2) and *Rasgrp1* (Ras-GRP) as measured by qRT-PCR are equivalently expressed in WT (LacZ) and *Nf1*^{-/-} (Cre) NSCs. There were no regional differences in the ratios of mRNA expression (KO/WT) of these regulators between CTX (white bars) and BS (black bars). **(B)** No change in the activation status of PKC α , S6K, S6 and 4EBP1 was observed in *Nf1*^{-/-} NSCs. In contrast, Akt activation was seen following neurofibromin loss in brainstem (BS), but not in cortex (CTX), NSCs. Values represent mean \pm SEM.